DNA Nanocapsules

DOI: 10.1002/anie.201302759

Controlled Release of Encapsulated Cargo from a DNA Icosahedron using a Chemical Trigger**

*Anusuya Banerjee, Dhiraj Bhatia, Anand Saminathan, Saikat Chakraborty, Shaunak Kar, and Yamuna Krishnan**

DNA is emerging as a powerful substrate for nanoconstruction.[1] Three dimensional (3D) polyhedra based on DNA have potential as "smart" delivery devices for molecular cargo in living systems.[2,3] A few reports have demonstrated the encapsulation of various molecular cargo within DNA polyhedra and their preliminary applications in cells and in vivo.[4,2b] However, to fully realize the potential of these polyhedra as carriers, a major challenge is the development of spatiotemporal release of the encapsulated cargo. If the cargo release process is coupled to the sensing of a given biomolecular signal, DNA polyhedra would then have the capacity to deliver a molecular payload in response to endogenous signals with both spatial and temporal control. Herein we demonstrate the controlled opening of a DNA icosahedron loaded with molecular cargo, in response to an external trigger, namely cyclic-di-GMP (cdGMP). cdGMP acts as a second messenger in bacteria and regulates processes such as signal transduction, response to the environment, transition from sessile to motile life forms and metabolism.[5]

We have designed a new chemically responsive DNA polyhedron **eI**, by integrating a well-characterized DNA icosahedron, **I** to a chemically responsive module that enables the opening of the nanocapsule in the presence of cdGMP. cdGMP aptamers have been incorporated into the icosahedral design to give rise to **eI**. In the presence of cdGMP, aptamer remodeling results in the dissociation of the **eI** into its two constituent halves by way of strand displacement. This releases the encapsulated internal cargo, namely fluorescent dextran. Using fluorescence spectroscopy to monitor the release of cargo, we achieved tight control over the opening of the DNA icosahedron and cargo release. Thus cargo-loaded polyhedra can be integrated with physiologically secreted molecular signals, which could provide spatial and/or temporal control over cargo release in diverse contexts.

We combined an aptamer that binds cdGMP into the overhangs of the upper half of the icosahedron $\mathbf{VU_5^{apt}}$ (Figure 1; Supporting Information, Figure S1), which is eventually combined with its cognate lower half ($\mathbf{VL_5}$) to form a new icosahedron **eI**, which is cdGMP responsive. **eI** was synthesized using a similar retrosynthetic strategy as published[4] with an alteration to the basic design of **U5WJ**, so that two cdGMP aptamers could be incorporated. This cdGMP aptamer is the ligand-sensitive module of the cdGMP riboswitch, derived from the class of GEMM riboswitches.[6] The ligand-bound form of the cdGMP aptamer (110Vc2) is structurally well characterized,[6,7] with a K_d of approximately 1 nM.[7] Importantly, the conformational change induced upon ligand binding has been determined with single-nucleotide resolution. Aptamer binding of cdGMP requires the formation of a duplex between its 5′ and 3′ ends (Figure 1a). We wanted to see whether this known conformational change could be used to drive a strand displacement reaction, in general, and on the icosahedral scaffold, in particular (Figure 1). If the conformational change of the cdGMP aptamer upon ligand binding could be coupled to a strand displacement reaction, then this design could be used to achieve ten simultaneous displacement reactions at ten independent sites on the icosahedron (Figure 1b, indicated

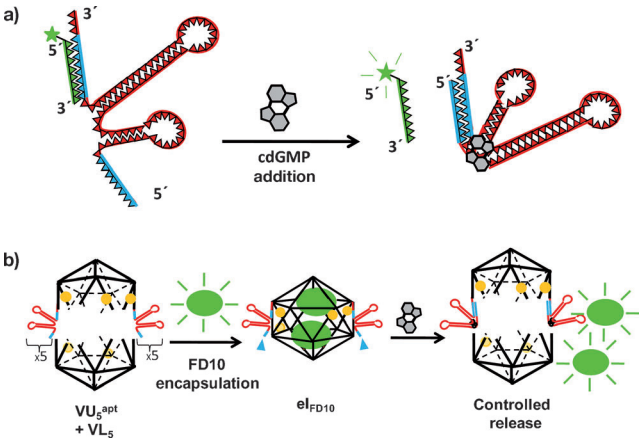

Figure 1. Design and incorporation of a ligand-sensitive module into a DNA icosahedron. a) Scheme of the conformational remodeling in the cdGMP aptamer upon binding of cdGMP to the aptamer. The apo-aptamer is annealed with a DNA strand (green). Upon ligand binding, the aptamer undergoes a conformational change and displaces the annealed strand into the solution. b) Scheme of the incorporation of the cdGMP aptamer into the icosahedron assembly to give controlled release of encapsulated cargo (FD10, green) upon addition of cdGMP. The aptamers (red/blue), fluorophores (yellow), and cdGMP (gray) are not drawn to scale.

[*] A. Banerjee, D. Bhatia, A. Saminathan, S. Chakraborty, S. Kar, Dr. Y. Krishnan
Biochemistry and Biophysics, National Centre for Biological Sciences, UAS-GKVK
Bellary Road, Bangalore (India)
E-mail: yamuna@ncbs.res.in

[**] We thank Harshavardhan Reddy, Bharath Raj, and Bharath Srikanth for valuable discussions. This work was presented in BIOMOD 2012 at the Wyss Institute, Boston (USA). This work was funded by NCBS. Y.K. thanks Wellcome Trust-DBT India Alliance for a Senior Research fellowship. D.B. thanks CSRI, GoI for a research fellowship.

Supporting information for this article is available on the WWW under http://dx.doi.org/10.1002/anie.201302759.

by cyan arrowheads). This would in turn result in the splitting of **eI** into its constituent halves in response to cdGMP (Figure 1b). If the icosahedral assembly was loaded with cargo, the dissociation of the icosahedral capsule could release the cargo into the bulk solution (Figure 1b). As a proof of principle, we show the release of an encapsulated fluorescent biopolymer, 10 kDa FITC dextran (FD10), from **eI** using cdGMP.

To determine if strand exchange could be coupled to the cdGMP aptamer folding on the nanocapsule scaffold, we used a hemi-icosahedron $\mathbf{eVU_5}$. $\mathbf{eVU_5}$ is a hemi-icosahedron with ten cdGMP aptamers, which upon binding cdGMP (as shown in Figure 1a), would require the duplexation of the 5′ to 3′ ends of the aptamers to undergo a conformational change. We performed a fluorescence de-quenching assay on $\mathbf{eVU_5}$. Hybridization of multiple FAM (fluorescein)-labeled 10-mer oligomers (FAM-10-mer) on $\mathbf{eVU_5}$, resulted in an increased local concentration of the FAM label on $\mathbf{eVU_5}$, yielding a self-quenched state for the FAM fluorescence.[8] If the cdGMP aptamers on $\mathbf{eVU_5}$ bind cdGMP and mediate a strand displacement reaction, it will cause an increase in fluorescence because of the increased distance between the displaced FAM labels in the bulk solution (Figure 2a; Supporting Information, Figure S5).

The upper half of the icosahedron ($\mathbf{eVU_5}$) was synthesized as described in Figures S1–S3. Furthermore, for this experiment, $\mathbf{eVU_5}$ was annealed with FAM-10-mer labels designed to be complementary to the 3′ end of the aptamer in a 1:10 ratio, to give rise to $\mathbf{eVU_5^{FAM}}$. When fluorescence intensities

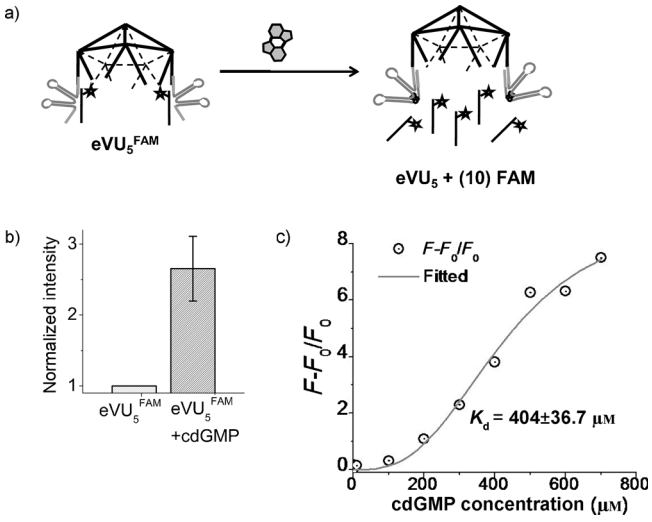

Figure 2. Strand displacement on $\mathbf{eVU_5}$ driven by cdGMP binding to an RNA aptamer: a) Scheme of cdGMP binding to a hemi-icosahedron pre-hybridized with ten FAM labels, $\mathbf{eVU_5^{FAM}}$. Binding of cdGMP causes displacement of ten pre-hybridized fluorescent DNA strands into solution increasing the fluorescent signal. b) Relief of self-quenching of pre-hybridized FAM labels on 100 nM $\mathbf{eVU_5^{FAM}}$ upon addition of 100 μM cdGMP. $n=3$, mean ± S.D. c) Efficiency of strand displacement on $\mathbf{eVU_5}$: 0–700 μM cdGMP was added to 100 nM $\mathbf{eVU_5}$ and the fluorescence intensity at a given cdGMP concentration was plotted relative to intensity in the absence of cdGMP at 32 °C with tetramethylrhodamine (TMR) as an internal control. Samples were excited at 488 nm and 547 nm and intensities were recorded at 515 nm and 596 nm for the FAM and TMR labels, respectively. FAM intensities of the samples were normalized to TMR intensities. $n=2$, mean ± S.D.

were recorded before and after addition of cdGMP, they showed a nearly three-fold increase relative to the initial, post-cdGMP addition (Figure 2b). This confirms that simultaneous strand displacement is indeed possible at ten independent sites on the hemi-icosahedral scaffold.

To determine the concentration regimes for operation of the aptamers attached to $\mathbf{VU_5^{apt}}$, we first determined the binding constant of $\mathbf{VU_5^{apt}}$ (K_d). We followed the binding by monitoring the increased fluorescence of FAM-10-mer owing to a decrease in self-quenching upon strand displacement. As shown in Figure 2c, the K_d value was found to be approximately 400 μM, significantly higher than that of the individual aptamer domain of the cdGMP riboswitch. The binding curve yielded a Hill coefficient of 1.85 indicating a cooperative release of FAM-10-mer molecules. This is consistent with previous results, where the formation of the icosahedron was also found to be highly cooperative.[4] The high, apparent K_d value of **eI** responsivity to cdGMP includes three processes—1) binding of cdGMP to its aptamer, 2) conformational change of the aptamer followed by 3) strand displacement (Supporting Information, Figure S8). Nevertheless, we observed that the cdGMP aptamer, when integrated into a 3D structure, retains its conformational response to cdGMP. Given that ten hybridized oligonucleotides can be simultaneously displaced upon cdGMP addition, we set out to test the displacement of the lower half of the icosahedron and to visualize this displacement by releasing encapsulated fluorescent cargo from the nanocapsule, **eI** (Supporting Information, Figures S1, S4). A fluorescently labeled cargo that is sensitive to collisional quenching was chosen to demonstrate cargo encapsulation. FD10 was encapsulated within **eI**, giving rise to $\mathbf{eI}_{FD10.}$ Encapsulation of FD10 inside **eI** was done by assembling **eI** in the presence of 2 mM of FD10 in an encapsulation buffer (10 mM phosphate buffer, pH 7.0, 100 mM NaCl, 1 mM $MgCl_2$). **eI** was subsequently purified from the unencapsulated FD10 and quantitated. Successful encapsulation of FD10 was demonstrated using a size-dependent quencher assay (Figure 3). The icosahedral nanocapsule has a pore size of 2.8 nm.[4] 4-Hydroxy-2,2,6,6-tetramethylpiperidine-1-oxyl (TEMPO-H) is about 1 nm in diameter and could permeate through the pores of **eI** and quench the encapsulated FD10. On the other hand, quenchers that are greater than 3 nm, (like the 6.2 nm gold nanoparticle (GNP)) did not quench the fluorescence of the encapsulated FD10. We obtained Stern–Volmer quenching constants (K_{SV}) for both TEMPO-H and 6.2 nm GNP on unencapsulated 100 nM FD10 (Supporting Information, Figure S7). Upon addition of $1/K_{SV}$ concentration of each of the quenchers to a solution of 50 nM unencapsulated FD10, the fluorescence intensity decreased by 50%. The fluorescence lifetime of FD10 encapsulated inside the icosahedron ($\mathbf{I}_{FD10}$) is similar to FD10 in solution.[2b] We used the same $1/K_{SV}$ concentration of each quencher on 50 nM $\mathbf{eI}_{FD10.}$ A similar decrease in fluorescence intensity was observed for $\mathbf{eI}_{FD10}$ to which TEMPO-H was added. However, when 6.2 nm GNP was added to $\mathbf{eI}_{FD10}$ the fluorescence intensity was largely unaffected.

To demonstrate cargo release upon opening of the icosahedron, **eI** was also functionalized with either five or

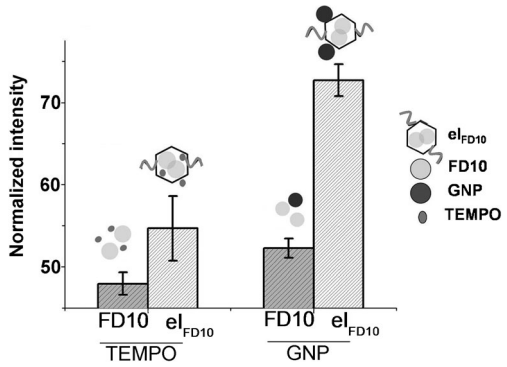

Figure 3. Encapsulation of fluorescent cargo FD10 inside **el** demonstrated by size-dependent fluorescence quenching. The fluorescence intensity of 50 nM unencapsulated FD10 and **el**$_{FD10}$ in the presence of 28 mM TEMPO-H or 0.25 nM of GNP is shown as a percentage of the initial fluorescence. Samples were excited at 488 nm and intensities recorded at 515 nm. $n = 3$, mean ± S.D.

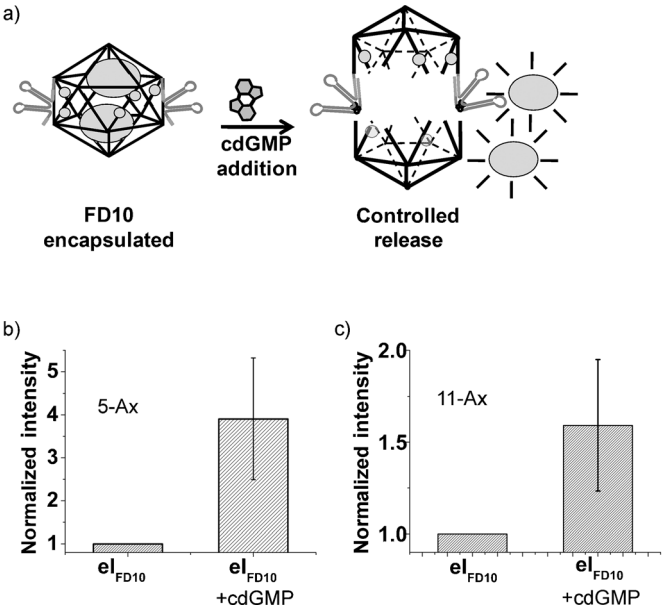

Figure 4. Release of encapsulated FD10 from **el**$_{FD10}$ mediated by cdGMP. a) Scheme of cargo release from the icosahedron **el**$_{FD10}$ modified with ten cdGMP aptamers (for clarity, only two aptamers are shown). **el**$_{FD10}$ was modified with either five (5-Ax) or eleven (11-Ax) Alexa-647 dye molecules as acceptors and FD10 molecules were encapsulated within. b–c) Ratio of donor (D) to acceptor (A) intensities of b) **el**$_{FD10}^{5\text{-Ax}}$ and c) **el**$_{FD10}^{11\text{-Ax}}$ before and after addition of 100 μM cdGMP. Samples were excited at 488 nm and the intensities were recorded at 515 nm (D) and 670 nm (A). $n = 3$, mean ± S.D.

eleven Alexa-647 fluorophores at well-defined locations on the nanocapsule. Given that fluorescein and Alexa-647 are a well-documented FRET pair,[9] the encapsulated FD10 could act as a donor fluorophore for FRET to a proximal Alexa-647 acceptor fluorophore localized on the body of the DNA icosahedron. Therefore in the encapsulated state, the donor intensity of fluorescein on FD10 is expected to be less, owing to host–cargo FRET. When the fluorescence of **el**$_{FD10}^{5-Ax}$ was recorded in the absence and presence of 100 μM cdGMP, addition of cdGMP caused a significant increase in the donor to acceptor fluorescence intensity (D/A) ratio (Figure 4b). This showed that the proximity of the FD10 to the Alexa-647 functionalized DNA icosahedron is lost upon release of FD10 into the bulk solution with cdGMP addition. This loss of host–cargo FRET is reflected in the increase in donor fluorescence. Similar results were obtained with an FD10-loaded, cdGMP-sensitive DNA icosahedron modified with eleven Alexa-647 fluorophores, (**el**$_{FD10}^{11-Ax}$; Figure 4c).

Thus, the addition of cdGMP that binds to the cdGMP aptamer of **el**$_{FD10}$ causes a conformational change in the aptamer at ten independent sites to induce strand displacement. This results in the dissociation of the lower half of the icosahedron **VL$_5$** from its upper half, **eVU$_5$**. This splits the icosahedron into its two constituent halves resulting in the controlled release of the encapsulated cargo. We have demonstrated the controlled opening of a cargo-loaded nanostructure in response to a chemical signal in bulk solution, with the concomitant release of its encapsulated molecular payload. The upper half of the icosahedral DNA scaffold was designed with cdGMP aptamers to produce a chemically responsive DNA polyhedron, **eI**. The well-characterized conformational change of cdGMP aptamers upon ligand binding was coupled, through strand displacement, to a large-scale structural change in the DNA icosahedron. The cascade of events (cdGMP binding leading to payload release) occurrs with a high apparent K_d and also lends additional insight into a perceived inconsistency in the naturally occurring cdGMP riboswitch, wherein the aptamer 110Vc2 has a K_d of approximately 1 nM.[7] The structural change upon cdGMP recognition stabilizes the P1 helix of the aptamer at its 3′ end (Supporting Information, Figure S8), which is crucial for cdGMP binding. However, it is still unclear whether the P1 helix exists in the apo-form of the riboswitch, implying a pre-organization of 110Vc2 for cdGMP binding,[10] or whether cdGMP binding induces P1 helix formation. In our system, the 3′ end of the aptamer is partially sequestered by a DNA oligonucleotide, abrogating P1 helix formation in the apo-state and leading to a dramatically increased K_d. Thus, this synthetic system supports the hypothesis that pre-organization of the P1 helix may facilitate the natural reaction cascades to occur at low micromolar cdGMP.

This chemically induced release strategy is applicable to other DNA polyhedra as well as for release of different molecular cargo. Given that the DNA icosahedron has been shown to deliver encapsulated cargo to specific cells in living organisms,[2b] our study delineates a system where it possible to now couple delivery and cargo release. The direct applications of stimulated cargo release from 3D DNA polyhedra are in the smart delivery of biologically important molecules in response to endogenous signals. This positions DNA polyhedra as intelligent nanovehicles for living systems.

Experimental Section

DNA icosahedra were constructed from three distinct five-way junction (5WJ) components **V**, **U^{apt}**, and **L**, with programmed

overhangs (Supporting Information, Table S1). Each 5WJ (**V**, $\mathbf{U}^{apt}$, and **L**) was constructed from equimolar ratios of the respective five 5′-phosphorylated single strands. 5WJ **V** formed a 1:5 complex with $\mathbf{U}^{apt}$ to give $\mathbf{VU_5}^{apt}$. The complementary module $\mathbf{VL_5}$ was synthesized from components **V** and **L** in a 1:5 ratio. Annealing of $\mathbf{VU_5}^{apt}$ and $\mathbf{VL_5}$ gave the chemically responsive icosahedron, **eI**. Encapsulation of cargo FD10 was carried out simultaneously with the annealing of $\mathbf{VU_5}^{apt}$ and $\mathbf{VL_5}$. Detailed synthetic and experimental methods are provided in the Supporting Information.[11–13]

Received: April 3, 2013
Published online: May 28, 2013

Keywords: aptamers · cargo release · DNA icosahedron · drug delivery · encapsulation

[1] a) Y. Krishnan, F. C. Simmel, *Angew. Chem.* **2011**, *123*, 3180 – 3215; *Angew. Chem. Int. Ed.* **2011**, *50*, 3124 – 3156; b) N. C. Seeman, *Annu. Rev. Biochem.* **2010**, *79*, 65 – 87.

[2] a) H. Lee et al., *Nat. Nanotechnol.* **2012**, *7*, 389 – 393; b) D. Bhatia, S. Surana, S. Chakraborty, S. P. Koushika, Y. Krishnan, *Nat. Commun.* **2011**, *2*, 339; c) D. Bhatia, S. Chakraborty, Y. Krishnan, *Nat. Nanotechnol.* **2012**, *7*, 344 – 346.

[3] a) F. A. Aldaye, A. L. Palmer, H. F. Sleiman, *Science* **2008**, *321*, 1795 – 1799; b) A. V. Pinheiro, D. Han, W. M. Shih, H. Yan, *Nat. Nanotechnol.* **2011**, *6*, 763 – 772; c) C. Zhang, Y. He, M. Su, S. H. Ko, T. Ye, Y. Leng, X. Sun, A. E. Ribbe, W. Jiangh, C. Mao, *Faraday Discuss.* **2009**, *143*, 221 – 233.

[4] D. Bhatia, S. Mehtab, R. Krishnan, S. S. Indi, A. Basu, Y. Krishnan, *Angew. Chem.* **2009**, *121*, 4198 – 4201; *Angew. Chem. Int. Ed.* **2009**, *48*, 4134 – 4137.

[5] a) R. Hengge, *Nat. Rev. Microbiol.* **2009**, *7*, 263 – 273; b) U. Römling, D. Amikam, *Curr. Opin. Microbiol.* **2006**, *9*, 218 – 228.

[6] N. Sudarsan, E. R. Lee, Z. Weinberg, R. H. Moy, J. N. Kim, K. H. Link, R. R. Breaker, *Science* **2008**, *321*, 411 – 413.

[7] K. D. Smith, S. V. Lipchock, T. D. Ames, J. Wang, R. R. Breaker, S. A. Strobel, *Nat. Struct. Mol. Biol.* **2009**, *16*, 1218 – 1223.

[8] a) X. Zhuang, T. Ha, H. D. Kim, T. Centner, S. Labeit, S. Chu, *Proc. Natl. Acad. Sci. USA* **2000**, *97*, 14241 – 14244; b) "Principles of Fluorescence Spectroscopy": J. R. Lakowicz, 3rd ed., Springer, Berlin, **2006**, pp. 69 – 70.

[9] J. Chen, A. Miller, A. L. Kirchmaier, J. M. Irudayaraj, *J. Cell Sci.* **2012**, *125*, 2954 – 2964.

[10] N. Kulshina, N. J. Baird, A. R. Ferré-D'Amaré, *Nat. Struct. Mol. Biol.* **2009**, *16*, 1212 – 1217.

[11] T. W. Kim, J. H. Park, J. I. Hong, *Bull. Korean Chem. Soc.* **2007**, *28*, 1221 – 1224.

[12] I. Gautier, M. Tramier, C. Durieux, J. Coppey, R. B. Pansu, J. C. Nicolas, K. Kemnitz, M. Coppey-Moisan, *Biophys. J.* **2001**, *80*, 3000 – 3008.

[13] E. Duchardt-Ferner, J. E. Weigand, O. Ohlenschläger, S. R. Schmidtke, B. Suess, J. Wöhnert, *Angew. Chem.* **2010**, *122*, 6352 – 6355; *Angew. Chem. Int. Ed.* **2010**, *49*, 6216 – 6219.

